

Fabrication of 15- μm Pitch 640×512 InAs/GaSb Type-II Superlattice Focal Plane Arrays

Fikri Oguz¹, Yetkin Arslan, Erkin Ulker, Alpan Bek, and Ekmel Ozbay¹

Abstract—We present the fabrication of large format 640×512 , 15- μm pitch, mid-wave infrared region (MWIR) InAs/GaSb type-II superlattice (T2SL) focal plane array (FPA). In this report, the details of device design and fabrication processes are withheld adhering to the common practice of most of the manufacturers and developers because of the strategic importance; however, information about fabrication processes of T2SLs FPA is presented to a certain extent. Comparison of etching techniques, passivation materials and methods, and substrate thinning (mechanical and chemical) is given besides of details regarding the standard ohmic contact and indium (In) bump formations. Morphological investigations of fabrication step are included. Large area pixels, $220 \mu\text{m} \times 220 \mu\text{m}$, fabricated by different etching methods and passivation materials/methods are compared in terms of dark current levels. Wet passivation with $(\text{NH}_4)_2\text{S}$ is discussed in terms of morphological investigations, and dark current results are compared with untreated samples. Large area pixel level characterizations as well as image level benchmarking of mechanical and chemical substrate thinning are reported. Effect of GaSb substrate on device performance and the way of reducing stress of In bumps are revealed. The importance of complete substrate removal is demonstrated through FPA images.

Index Terms—Fabrication, focal plane array, infrared photodetectors, mid-wave infrared region, type-II superlattice.

I. INTRODUCTION

AN INFRARED device is fabricated by executing consecutive process steps that start with epilayer growth. Fabrication steps being well-established and feasible plays a decisive role in the performance of a device. Therefore, research groups and developers work constantly for reaching optimum fabrication processes in order to fabricate highly qualified sensors. For InAs/GaSb T2SLs, FPA fabrication is

the hottest topic for infrared researchers because of their promising performance which is comparable to that of the mature binary (e.g. InSb), ternary (e.g. HgCdTe) compound semiconductors as well as quantum structured devices such as quantum well infrared photodetectors (QWIPs). There are different types of approaches for the fabrication of T2SL FPAs. Both wet etching and dry etching methods are utilized for fabrication of mesa type FPA structures. Some etchants for GaSb and InAs are reported in the literature [1]. Also, mixture of phosphoric (H_3PO_4) and citric ($\text{C}_6\text{H}_8\text{O}_7$) acid solutions is an alternative etchant for T2SL [2]. The mixing ratio for $\text{C}_6\text{H}_8\text{O}_7/\text{H}_2\text{O}:\text{H}_2\text{O}_2$ changes the etch rate of the solution [3]. Although most of the research groups and developers prefer wet etch in mesa formation, a few of them use dry etching in mesa formation step [4]. Different types of gas mixtures are used in dry etching of InAs/GaSb T2SLs such as chlorine based [5], CH_4 based [6], and halogen gas mixtures [7]. For the formation of ohmic contact, Ti, Pt, and Au are used as ohmic contact metals by many groups [4], [8]. Among other FPA fabrication steps, passivation can be regarded as the most performance affecting one because inadequate surface passivation is a severely performance limiting factor. Therefore, the general trend for this step is to keep details as proprietary information by detector manufacturers. Large number of passivation methods and materials are available in the literature for T2SL structures, including dielectric coatings and electrochemical deposition without details. However, most of the manufacturers and researchers agree with using SiO_2 as a passivation material. Some researchers and developers use additional treatment before passivation. Some groups examine ammonium sulfide treatment, and it is sometimes called ‘wet passivation’ [9], [10]. Their claims involve an explanation that broken bonds tie with sulfide, and the surface is sulfurized instead of being oxidized; as a result of this, some improvement is attained in device performance.

InAs/GaSb T2SLs are usually grown on GaSb because of close lattice constants of substrate GaSb and epilayer. Backside illumination of hybridized FPA - readout integrated circuit (ROIC) can cause serious problems. Relatively large absorption caused by GaSb substrate in infrared region decreases the sensitivity of the device [11]. Moreover, difference in-between thermal expansion coefficients of Si ROIC and T2SL FPA reduces the reliability of FPA due to stress applied to In bumps at operation-temperatures below 100 K. Therefore, the substrate should be thinned or removed to avoid these problems. Substrate thinning process is hard to operate due to the fragile nature of both T2SL FPA and Si ROIC, which is

Manuscript received January 7, 2019; revised April 25, 2019; accepted May 17, 2019. Date of publication May 29, 2019; date of current version June 20, 2019. (Corresponding author: Fikri Oguz.)

F. Oguz is with the Micro and Nanotechnology Graduate Program, Middle East Technical University (METU), 06800 Ankara, Turkey, and also with the Nanotechnology Research Center, NANOTAM, Bilkent University, 06800 Ankara, Turkey (e-mail: fikri@metu.edu.tr).

Y. Arslan and E. Ulker are with FOTONIKA Co., 06810 Ankara, Turkey (e-mail: yetkin@fotonika.com.tr; erkin@fotonika.com.tr).

A. Bek is with the Micro and Nanotechnology Graduate Program, Middle East Technical University (METU), 06800 Ankara, Turkey, and also with the Department of Physics, Middle East Technical University (METU), 06800 Ankara, Turkey (e-mail: bek@metu.edu.tr).

E. Ozbay is with the Nanotechnology Research Center, NANOTAM, Bilkent University, 06800 Ankara, Turkey, also with the Department of Physics, Bilkent University, 06800 Ankara, Turkey, and also with the Department of Electrical and Electronics Engineering, Bilkent University, 06800 Ankara, Turkey (e-mail: ozbay@bilkent.edu.tr).

Color versions of one or more of the figures in this paper are available online at <http://ieeexplore.ieee.org>.

Digital Object Identifier 10.1109/JQE.2019.2919771

GaSb:Be, Contact p+ Layer, 0.30 μm , $N_A \sim 3 \times 10^{18}$
InAs/GaSb: Be, p Layer, 0.40 μm , $N_A \sim 2 \times 10^{17}$
InAs/GaSb, i Absorber Layer, 1.50 μm
i Barrier Layer, 0.40 μm
InAs/GaSb:Si, N+ Contact, 0.40 μm , $N_D \sim 2 \times 10^{17}$
InAs _(x) Sb _(1-x) :Si, Etch stop, 1.00 μm , $N_D \sim 1 \times 10^{18}$
GaSb Buffer Layer, 0.20 μm , nid
N-GaSb Substrate

Fig. 1. piBn epilayer structure (not scaled).

relatively more rigid than FPA. There are some methods used in literature for substrate thinning such as lapping, grinding and chemical etching.

Here, we present a large format $640 \times 512 \times 15 \mu\text{m}$ pitch MWIR InAs/GaSb T2SL FPA fabrication. The detector has cut-off wavelength at $4.9 \mu\text{m}$. Mesa type structure is adopted for T2SL FPA. Ohmic contacts are formed by using Ti/Au metals. We have, also, tested non-treated SiO_2 deposition and ammonium sulfide pre-treated SiO_2 deposition for passivation besides with other methods/materials. Mechanical grinding and chemical etching based two-step substrate removal approach is used.

II. FABRICATION OF T2SL FPA

The superlattice used for this study has piBn band structure grown on GaSb substrate with heavily doped GaSb cap layer which makes to get contact easier. With this piBn structure, it is aimed to utilize relatively higher mobility of electrons for collection efficiency of p-type absorber layer. Also, by adding barrier layer into a structure provides opportunity to reduce surface leakages. The InAsSb etch stop layer is adopted to use etch selectivity of InAsSb and GaSb which will be detailed in substrate removal part. Also, GaSb buffer layer is included in structure to make transitions from substrate to epilayer easier. The epilayer structure is given in Fig.1.

T2SL detector is fabricated in mesa-type. The common approach for mesa-type detector fabrication is centered on wet and dry etching of epilayer surfaces.

In our work, combinations of $\text{C}_6\text{H}_8\text{O}_7/\text{H}_2\text{O}:\text{H}_3\text{PO}_4:\text{H}_2\text{O}_2$ at a ratio of 10:1:1 is examined for suitability as a wet etching recipe for T2SL structures. Various $15 \mu\text{m}$ pitch samples are prepared using fixed lithography parameters on pieces of the same wafer on which etching experiments are performed. The etch rate is calculated as 8 nm/s. To investigate the smoothness of mesa sidewalls and surface, SEM images are taken (Fig. 2).

As seen in Fig.2, the step in etched structure is observed at the top of mesas. This is because of the etching profile and rate of heavily doped GaSb cap layer, the upmost layer in epi-structure, have different etch rate than following p contact, absorbing, barrier and n contact layers. Moreover, because of the isotropic feature of wet etch method, the sidewall inclination is not at ultimate configuration point but it is possible to passivate these sidewalls with these

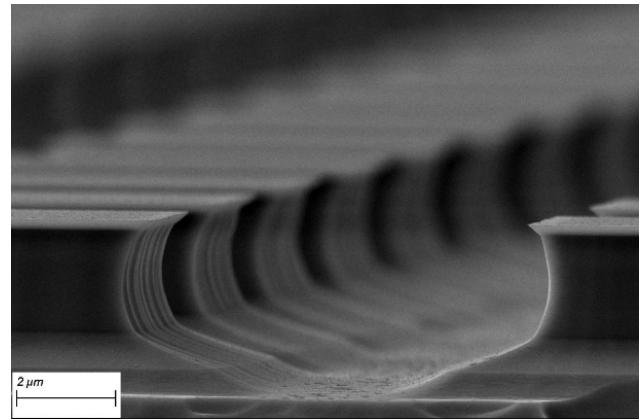


Fig. 2. SEM image of mesa etched sample with $\text{C}_6\text{H}_8\text{O}_7/\text{H}_2\text{O}:\text{H}_3\text{PO}_4:\text{H}_2\text{O}_2$ at a ratio of 10:1:1.

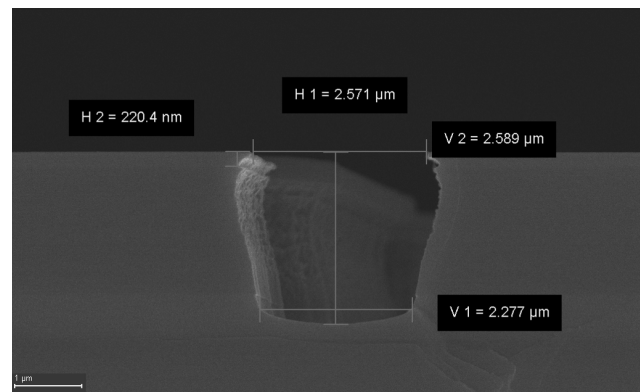


Fig. 3. The optimized dry etching recipe results in mesa structures with flat overcut sidewalls.

inclinations. Also, the sidewalls seem to be rough from SEM image. This mainly because of the differentiating InAs, GaSb, InSb, and AlSb layers in epilayer structures which have relatively different etching rate and etching profile against $\text{C}_6\text{H}_8\text{O}_7/\text{H}_2\text{O}:\text{H}_3\text{PO}_4:\text{H}_2\text{O}_2$ solution. For the same reason, we observe such roughness in dry etched sample like shown in Fig.3. For dry etching, a chlorine-based mixture (BCl_3/Cl_2) followed by a post-treatment procedure is studied for dry etching of T2SLs. Proper mixing ratio for BCl_3 , Cl_2 , and Ar is established after several experiments for optimizing etch rate and etching profile. After carefully determining appropriate ion densities and energies in light of carefully conducted trials, a dry etching recipe for T2SLs is obtained. The final optimization is performed on sidewall morphologies. Fig. 3 shows an SEM image of a sample with mesa structure obtained by the final optimized dry etch recipe.

Even if the shape of mesa walls are optimized, the damage caused by dry etch can be easily observed which seems more than in wet etched case. To investigate the effect of damage on device performance in terms of dark current density, two large-area-pixel detectors with same size mesas are fabricated with dry and wet etching methods for comparison. While an optimized gas mixture of BCl_3 , Cl_2 , and Ar together with Ar plasma post-treatment step is used for dry etching, $\text{C}_6\text{H}_8\text{O}_7/\text{H}_2\text{O}:\text{H}_3\text{PO}_4:\text{H}_2\text{O}_2$ solution with a ratio of 10:1:1 is

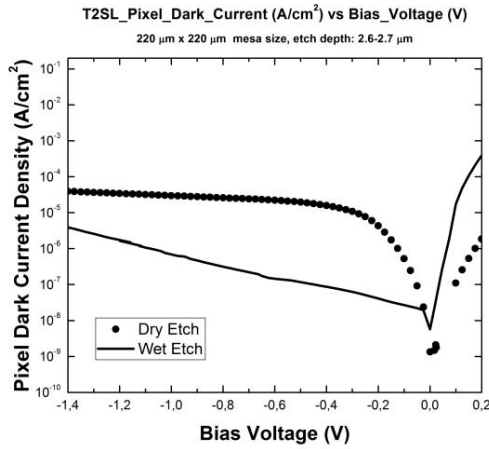


Fig. 4. 77 K dark current densities of $220 \mu\text{m} \times 220 \mu\text{m}$ pixel area samples for dry and wet etched samples.

used for wet etching. Samples are etched up to $2.6 - 2.7 \mu\text{m}$ depth. The same ohmic contact formation procedure is applied to both samples. I-V measurements are performed at 77 K in dewar. The results are presented in Fig. 4.

While wet etched sample gives $1.3 \times 10^{-11} \text{A}$ dark current at -0.1V bias, $2.5 \times 10^{-10} \text{A}$ dark current obtained at same bias voltage for dry etched sample. Although dark currents of the two samples coincide at around -0.05V bias voltage, dark current of dry etched sample is up to 2 orders of magnitude larger than wet etched sample. Also, after measuring the I-V characteristic of dry etched sample, it is dipped in $\text{C}_6\text{H}_8\text{O}_7/\text{H}_2\text{O}:\text{H}_3\text{PO}_4:\text{H}_2\text{O}_2$ solution to reduce ion damage occurring especially in mesa sidewalls. After this process, I-V measurements are performed again. However, no enhancement is recorded. The results are exactly same with the previous results. Therefore, in order not to complicate I-V graph, it is omitted. After these investigations, it is sure to state that more enhancement is needed for optimum dry etching to suppress dark current besides with damage-free mesa walls. Thus, wet etching is preferred for further investigations.

In the following step, the ohmic contacts are deposited with e-beam evaporation as a combination of thin Ti/Au metals. Various passivation methods and materials are used including SiO_2 deposition with plasma enhanced chemical vapor deposition (PECVD) and e-beam evaporation techniques, polyimide coating with and without curing, and photoresist coating. They are compared in terms of I-V characteristics, measured on large pixel area samples (Fig. 5). All samples are fabricated with the same procedure. The only difference between them is the passivation method or material.

Dark currents for all methods are almost at the same level. To illustrate, cured polyimide passivated sample yields $1.5 \times 10^{-11} \text{A}$ dark current whereas PECVD SiO_2 passivated samples gives $1.3 \times 10^{-11} \text{A}$ at same bias voltage of -0.1V . It is also observed that polyimide gives relatively lower dark current result regardless of being cured or uncured. Its ability to yield low dark current makes polyimide the better choice for passivation material. Also, polyimide provides opportunity to compensate this wavy surface. In other words, it provides surface planarization besides with conformal coating.

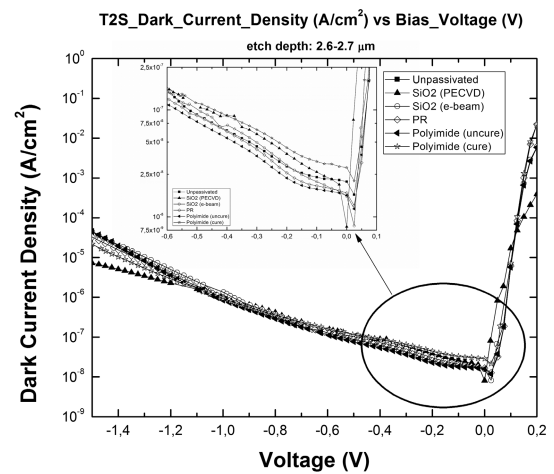


Fig. 5. The dark current density comparison of different passivation methods/materials at 77 K.

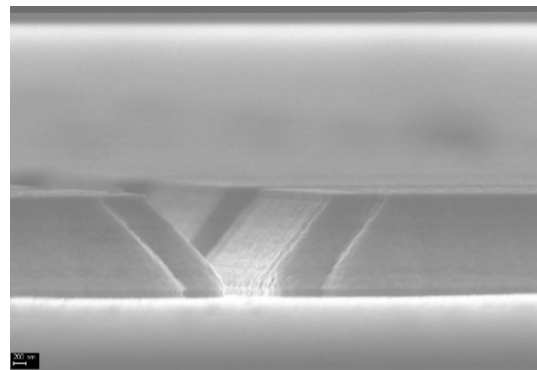


Fig. 6. SEM image of $(\text{NH}_4)_2\text{S}$ treated mesas.

Another investigation on passivation was made by pre-treatment of the mesa surface by ammonium sulfide ($(\text{NH}_4)_2\text{S}$) before SiO_2 deposition. For this purpose, $(\text{NH}_4)_2\text{S}$ is diluted in H_2O at a ratio of 1:20 ($(\text{NH}_4)_2\text{S}:\text{H}_2\text{O}$) and etched samples with mesa formations were soaked in this solution for 2 minutes. An SEM image of such post-treated mesas is given in Fig. 6.

By this way, neither morphological improvement is observed after $(\text{NH}_4)_2\text{S}$ treatment nor the mesa walls are damaged. Positive effect of this pre-treatment step on device performance is, however, indicated in literature [10]. For this reason, two pieces of large-pixel-size samples are fabricated that differ from each other only with $(\text{NH}_4)_2\text{S}$ pre-treatment. So, among other passivation methods, we compared $(\text{NH}_4)_2\text{S}$ pre-treated plus PECVD SiO_2 coated and SiO_2 coated samples which are etched away with $\text{C}_6\text{H}_8\text{O}_7/\text{H}_2\text{O}:\text{H}_3\text{PO}_4:\text{H}_2\text{O}_2$ solution (Fig. 7.). Before comparing them, pre-treated pieces were coated with SiO_2 films deposited at different temperatures starting from 250°C , 230°C , 200°C , and 180°C , respectively. The deposition temperature is reduced slightly since high temperature can damage the sulphide bonds and this can affect diode performance. After each deposition, I-V measurements are performed. The best result is obtained with SiO_2 deposited at 200°C . After these investigations, the pre-treated sample

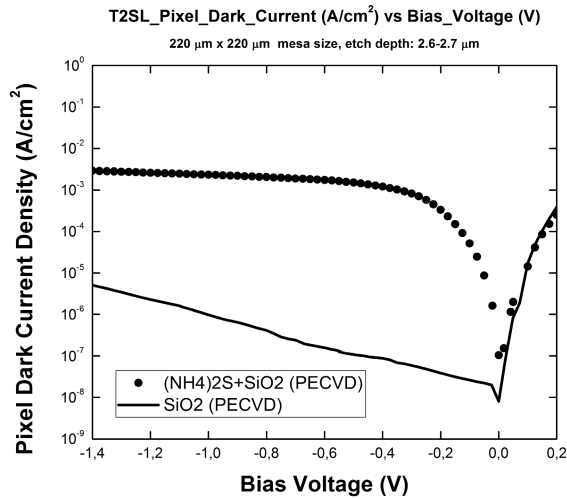


Fig. 7. 77 K dark current densities of $220 \mu\text{m} \times 220 \mu\text{m}$ pixel area $(\text{NH}_4)_2\text{S}$ pre-treated and non-treated samples with PECVD SiO_2 .

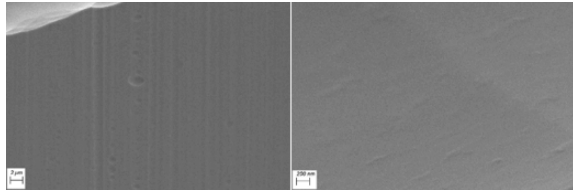


Fig. 8. SEM images of the grinded substrate.

is found to produce a 2×10^3 times higher dark current than non-treated SiO_2 coated sample.

Following the passivation step, the FPA fabrication continues with under bump metallization by deposition of Ti/Ni/Au metal layer by using e-beam evaporation. Next, indium (In) bumps are deposited on pixels by thermal evaporation. After dicing the FPA samples according to ROIC necessities, FPAs are hybridized with ROICs and underfilling epoxy is injected. Afterwards, the GaSb substrate is completely removed in two steps; first by mechanical thinning of the substrate around several hundreds of μm by grinding and then by selective chemical etching. The substrate of T2SL FPA is thinned by grinding to a thickness below $50 \mu\text{m}$. The starting thickness of the GaSb substrate is $625 \pm 15 \mu\text{m}$ in our case. The SEM images of grinded GaSb substrate are provided in Fig. 8.

A chemical etching of the substrate is performed after grinding it down to around $50 \mu\text{m}$ thickness. $\text{CrO}_3:\text{HF}:\text{H}_2\text{O}$ with a ratio of 23:1:1 is used as a chemical etchant in this process. The etch rate is $\sim 1.8 \mu\text{m}/\text{min}$. The selectivity of this etchant in between GaSb and InAsSb is around 1:100 (InAsSb:GaSb). The mixing ratio can be adjusted for faster etching. In this step, the remaining thickness of the substrate is completely removed by chemical etching. In case it is not removed, photoabsorption in the GaSb substrate causes a decrease of the number of photons reaching the active layer. Furthermore, GaSb substrate also leads to crosstalk shown in images. In Fig. 9, 77 K imaging performance of a dummy FPA is demonstrated. The substrate of this FPA is thinned but a $\sim 50 \mu\text{m}$ thick portion remains. The image



Fig. 9. An image acquired by FPA having a $50 \mu\text{m}$ thick substrate.

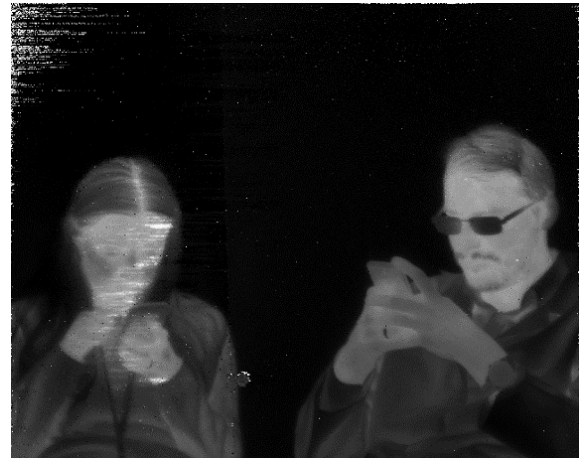


Fig. 10. An image acquired by FPA having completely removed substrate.

is acquired with $f/2.3$ optics and 2 ms integration time. Upper left-hand-side of FPA is damaged during grinding cycle, and it has large void defects in the middle. The crosstalk effect of the remaining GaSb substrate can easily be noticed. When FPA is un-mounted, it is observed that FPA is cracked most probably at the cooling cycle. Although such cracks are a serious problem, it has allowed us to investigate the substrate visually.

Afterwards, the $50 \mu\text{m}$ thick GaSb substrate is completely removed with chemical etching. An image is acquired in same conditions. In Figure 10, the image acquired by the same FPA with completely removed substrate is given.

From the image, it can be discerned that there have been adverse effects of chemical substrate removal. The chemical etchant is found to attack FPA at defects and cracks. At several positions, additional irresponsive pixels are observed. However, the crosstalk of the image disappears although image seems not to be better than other in initial look. This crosstalk is mainly caused by polishing of GaSb substrate. When the substrate are thinned by grinding, the surface of grinded substrate includes scratches and voids. These scratches should scatter light and introduce an optical crosstalk. Therefore, after thinning the substrate at reasonable thickness which

decreases the stress on detector mainly caused by the thermal expansion coefficients of Si ROIC and InAs/GaSb detector on GaSb substrate, the surface of substrate should be polished. According to the goodness of polishing crosstalk issue can be overcome. However, in our case, polishing of the substrate are not desired level. Thus, we have completely removed GaSb substrate with chemical etching besides with reducing stress in between substrate and ROIC. This comparison shows that GaSb substrate creates crosstalk in FPA image, therefore, it should be removed entirely in T2SL detectors for better performance if polishing is not operated well.

III. CONCLUSION

The important steps of fabrication of 640 \times 512 MWIR T2SL FPA are investigated in this paper. The p-i-B-n layer is etched for mesa type pixel formation. Both wet and dry etching methods are tested. However, the $\text{C}_6\text{H}_8\text{O}_7/\text{H}_2\text{O}:\text{H}_3\text{PO}_4:\text{H}_2\text{O}_2$ solution yields better results than BCl_3/Cl_2 based dry etching based on device performance. Dry etching process requires to be improved further for being deemed suitable. The effect of surface pre-treatment with $(\text{NH}_4)_2\text{S}$ just before SiO_2 passivation coating is compared to non-treated SiO_2 passivation in terms of dark current densities. And $(\text{NH}_4)_2\text{S}$ step is found to be developed. A two-step substrate removal process is applied and morphologically analyzed. CrO_3 based chemical etchant with its highly selective nature between GaSb substrate and InAsSb etch-stop layer provides opportunity to remove substrate completely. However, it is found that the applicability of this selective chemical substrate removal step is limited by the presence of defects.

REFERENCES

- [1] O. Dier, C. Lin, M. Grau, and M.-C. Amann, "Selective and non-selective wet-chemical etchants for GaSb-based materials," *Semicond. Sci. Technol.*, vol. 19, no. 11, pp. 1250–1253, 2004.
- [2] R. Chaghi, C. Cervera, H. Ait-Kaci, P. Grech, J.-B. Rodriguez, and P. Christol, "Wet etching and chemical polishing of InAs/GaSb superlattice photodiodes," *Semicond. Sci. Technol.*, vol. 24, no. 6, May 2009, Art. no. 065010.
- [3] K.-M. Chang, J.-J. Luo, C.-D. Chiang, and K.-C. Liu, "Wet etching characterization of InSb for thermal imaging applications," *Jpn. J. Appl. Phys.*, vol. 45, pp. 1477–1482, Mar. 2006.
- [4] E. Plis *et al.*, "nBn based infrared detectors using type-II InAs/(In,Ga)Sb superlattices," *Proc. SPIE*, vol. 6940, May 2008, Art. no. 69400.
- [5] F. Rutz *et al.*, "InAs/GaSb superlattice focal plane array infrared detectors: Manufacturing aspects," *Proc. SPIE*, vol. 7298, May 2009, Art. no. 72981R.
- [6] L. Yang, J. Deng, Y.-L. Shi, Y.-Y. Chen, and B. Wu, "Fabrication and performance of InAs/GaSb type-II superlattices mid-wavelength infrared detectors," *Proc. SPIE*, vol. 8907, Sep. 2013, Art. no. 890741.
- [7] H. Inada *et al.*, "Pretreatment for surface leakage current reduction in type-II superlattice MWIR photodetectors," *Proc. SPIE*, vol. 9070, Jun. 2014, Art. no. 90700Z.
- [8] H. Katayama *et al.*, "Development of type II superlattice detector for future space applications in JAXA," in *Proc. Conf. Lasers Electro-Opt. Pacific Rim (CLEOPR)*, vol. 8353, Jun./Jul. 2013, pp. 1–8.
- [9] A. Gin, Y. Wei, J. Bae, A. Hood, J. Nah, and M. Razeghi, "Passivation of type II InAs/GaSb superlattice photodiodes," *Thin Solid Films*, vols. 447–448, pp. 489–492, Jan. 2004.
- [10] A. Gin *et al.*, "Ammonium sulfide passivation of type-II InAs/GaSb superlattice photodiodes," *Appl. Phys. Lett.*, vol. 84, pp. 2037–2039, Jan. 2004.
- [11] K. Miura, Y. Iguchi, T. Katsuyama, and Y. Kawamura, "Mid-infrared sensors with InAs/GaSb superlattice absorption layers grown on InP substrates," *SEI Tech. Rev.*, vol. 1, no. 78, pp. 58–62, Apr. 2014.



Filkri Oguz received the B.Sc. degree from the Department of Physics, Middle East Technical University, Ankara, Turkey, and the M.Sc. degree from the Department of Micro and Nanotechnology, Middle East Technical University. He is currently a Research Engineer with the Nanotechnology Research Center (NANOTAM), Bilkent University. His research interests include growth, fabrication, and characterization of infrared sensor arrays.



Yetkin Arslan received the B.Sc., M.Sc., and Ph.D. degrees from the Department of Electrical and Electronics Engineering, Middle East Technical University, Ankara, Turkey. He is currently one of the co-founders of FOTONIKA Co. His research interests include growth, fabrication, and characterization of infrared sensor arrays based on III–V and II–VI compound semiconductors.



Erkin Ulker received the B.Sc. and M.Sc. degrees from the Department of Electrical and Electronics Engineering, Hacettepe University, Ankara, Turkey. He is currently one of the co-founders of FOTONIKA Co. His research interests include growth, fabrication, and characterization of infrared sensor arrays based on III–V and II–VI compound semiconductors.



Alpan Bek received the B.Sc. and M.Sc. degrees from the Department of Physics, Bilkent University, and the Ph.D. degree from the Department of Physics, Swiss Federal Institute of Technology (EPFL), Lausanne, Switzerland, and the Max-Planck Institute for Solid State Research, Stuttgart, Germany. He is currently an Associate Professor with the Department of Physics and Micro and Nanotechnology, Middle East Technical University, Ankara, Turkey. His research interests include plasmonics, tip-enhanced Raman spectroscopy (TERS), near field optics, apertureless scanning near field optical microscopy (aSNOM), scanning probe spectro-microscopy, lightwave information technology, integrated and fiber optics, electro- and acousto-optics, semiconductors and fabrication, and characterization of infrared sensor arrays.



Ekmel Ozbay received the B.S. degree in electrical engineering from Middle East Technical University, Ankara, Turkey, in 1983, and the M.S. and Ph.D. degrees in electrical engineering from Stanford University in 1989 and 1992, respectively. He was a Post-Doctoral Research Associate with Stanford University from 1992 to 1993, where he was involved in high-speed resonant tunneling and optoelectronic devices. From 1993 to 1995, he was a Scientist with the DOE Ames National Laboratory, Iowa State University, in the area of photonic bandgap materials. In 1995, he joined Bilkent University, Ankara, where he is currently a Full Professor with the Physics Department and the Department of Electrical and Electronics Engineering. He is also the Director of the Nanotechnology Research Center, Bilkent University, where he is involved in nanophotonics, nanometamaterials, nanoelectronics, nanoplasmonics, nanodevices, photonic crystals, GaN/AlGaN MOCVD growth, fabrication and characterization of III–V compound semiconductors, GaN-based devices, and high-speed optoelectronics.